Third International Conference on Motion and Vibration Control, Chiba, September, 1-6, 1996

Warp Control of a Silicon-Wafer Slicer Cutting a Crystal Ingot

K. Masui [*1], S. Chonan [*2] and Z. W. Jiang [*2]

[*1] Manufacturing Systems Department
Mechanical Engineering Laboratory, Tsukuba, Japan

[*2] Department of Mechatronics and Precision Engineering
Tohoku University, Sendai, Japan

Abstract

The analysis of warp control for a silicon wafer slicer in cutting a crystal ingot is presented in this paper. The rotating sawblade is clamped at the outer periphery and stressed initially in the radial direction, while the inner periphery is subjected to stationary in-plane and quasi-static lateral slicing loads from the workpiece. Further, pneumatic normal forces are applied to the blade to suppress the warp of blade. The blade deflection is obtained analytically by applying the multi-modal expansion and the Galerkin method to the governing equations of system. Numerical results are presented for an actual blade cutting an 8″-diameter silicon ingot at a speed of 1150 rpm. An integral algorithm is introduced to control the pneumatic forces applied to the rotating blade. Results obtained show that the warp of blade is reduced effectively by the control forces applied to the locations outside the path of the sliced ingot. In addition, the deflection at the center of cutting edge is suppressed and the flatness of blade is improved due to the pneumatic moment applied to the blade.

1. Introduction

The ID (inner-diameter) saw blade is nowadays commonly used in the crystal wafering. Demands on large-diameter silicon wafer have accelerated the development of the large-scale ingot slicer, whith which silicon wafers with adequately flat, parallel sides can be produced for high performance of the IC devices. To meet these requirements both for the slicer and for the wafer, new active control methodologies are needed for a highly efficient slicer.

Several papers have been published in recent years on the vibration and control of rotating disks. Ellis et al. [1] analyzed a feedback vibration controller that increases the transverse stiffness and damping of a circular OD (outer-diameter) saw. Radcliffe et al. [2] used an on-line FFT analysis of the rotating disk displacement to suppress the amplitude of the dominant mode. Hutton et al. [3] analyzed the response of OD sawblade with stationary point springs. Huang et al. [4] investigated a circular line guide system to increase the critical speed of a spinning annular plate. Chonan et al. [5] obtained the in-plane stress distribution in a silicon-wafer slicer cutting a crystal ingot taking into account all stresses from the spinning, the initial tensioning in the radial direction and the in-plane reaction from the workpiece. Further study on the natural vibration of the rotating ID saw with the in-plane stresses and obtained the deflection of the blade subjected to the static lateral cutting force has also been reported [6].

The warp of the wafer produced during the cutting process is the locus of the cutting edge of the ID sawblade. However, the warp control of the ID sawblade slicing a crystal ingot have not been studied.

In this paper, the response of an ID sawblade

slicing a crystal ingot is studied analytically to reduce the warp of the wafer. Numerical results are presented for an actual blade cutting an 8″-diameter silicon ingot at a speed of 1150 rpm. The air control forces applied to the blade are approximated by concentrated forces. Effects on the blade deflection of the air control forces are studied in detail.

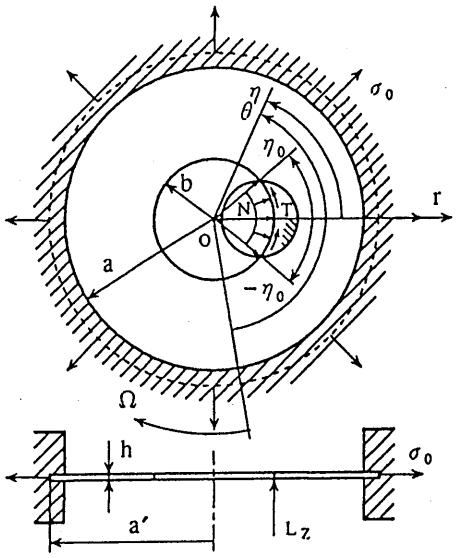

Fig.1 The coordinate system for a rotating silicon-wafer slicer. The sawblade is clamped at the outer periphery while the inner periphery is subjected to the cutting load.

2. Formulation and Analysis

Figure 1 shows an ID saw blade slicing a silicon ingot at a constant angular speed Ω. The blade has a thickness h and is free at the inner edge ($r = b$). After initially tensioned in the radial direction by the radial stress σ_0 along the outer periphery $r = a'$, the blade is clamped from both sides by two rigid rings on the range $a \leq r \leq a'$. In the figure, the system (r,θ) is a co-ordinate frame rotating with the blade, while the (r,η) another frame fixed in space. The cutting force is decomposed into in-plane radial compressive force N (Pa), circumferential shear force T (Pa) and axial lateral force L_z (N). Each of them is assumed uniformly distributed over the arc $|\eta| \leq \eta_0$ along the inner periphery of blade. The lateral cutting force $g(r,\eta,t)$ acting on the blade is generally represented by

$$g(r,\eta,t) = \sum_{k=1}^{K} q(t)(1/r)\delta(r - r_k)\delta(\eta - \eta_k), \qquad (1)$$

where $\delta(\ )$ is the Dirac delta function and K is the total number of concentrated lateral forces assumed. The problem discussed in the following is the effect on the blade deflection of the air control forces applied to the blade. The air pressure to control the blade deflection is approximated by lateral concentrated forces applied to the blade. These control forces are written in the form

$$s(r,\eta,t) = \sum_{k=1}^{K_c} f_k(t)(1/r)\delta(r - r_k)\delta(\eta - \eta_k), \qquad (2)$$

where K_c is the number of the control forces.

The equation governing the deflection of the blade referred to the co-ordinate frame fixed in space is

$$\begin{aligned} &D[\partial^2/\partial r^2 + (1/r)\partial/\partial r + (1/r)^2\partial^2/\partial\eta^2]^2 w \\ &\quad +\rho h[\partial/\partial t - \Omega\partial/\partial\eta]^2 w \\ &\quad -h[(1/r)\partial/\partial r(r\sigma_r\partial w/\partial r) \\ &\quad +(1/r^2)\partial/\partial\eta(\sigma_\eta\partial w/\partial\eta) \\ &\quad +(1/r)\partial/\partial r(\tau_{r\eta}\partial w/\partial\eta) \\ &\quad +(1/r)\partial/\partial\eta(\tau_{r\eta}\partial w/\partial r)] \\ &\quad = g(r,\eta,t) + s(r,\eta,t), \end{aligned} \qquad (3)$$

where $w(r,\eta,t)$ is the lateral displacement of the blade, $D(= Eh^3/12(1-\nu^2))$ is the flexural rigidity, E is the Young's modulus, ν is the Poisson's ratio and ρ is the mass density of blade; σ_r is the in-plane radial normal stress, σ_η the hoop stress, and $\tau_{r\eta}$ the shear stress in the rotating blade, which are presented in Reference [5].

One assumes the solution of equation (3) in the Fourier series as

$$\begin{aligned} w(r,\eta,t) = \sum_{m=0}^{M}\sum_{n=0}^{N} &[C_{mn}(t)\cos(n\eta) \\ &+S_{mn}(t)\sin(n\eta)]R_{mn}(r). \end{aligned} \qquad (4)$$

Here, R_{mn} is the mode function of a non-rotating stationary blade clamped along the outer boundary ($r = a$) while free at the inner edge ($r = b$); m and n are the numbers of nodal circles and diameters on the blade. R_{mn} is given by

$$\begin{aligned} R_{mn}(r) = &\mathrm{J}_n(k_{mn}r) + F_{mn}\mathrm{Y}_n(k_{mn}r) \\ &+G_{mn}\mathrm{I}_n(k_{mn}r) + H_{mn}\mathrm{K}_n(k_{mn}r), \end{aligned} \qquad (5)$$

where J_n and Y_n are the Bessel functions of the first and second kinds, and I_n and K_n are the modified Bessel functions; F_{mn} through H_{mn} and k_{mn}'s are the unknowns and eigenvalues determined from the boundary conditions of the blade.

Substituting equation (4) into equation (3), further applying the Galerkin method to the resulting equation, one has a system of simultaneous ordinary differential equations of the form

$$M\ddot{X} + \Gamma\dot{X} + KX = Qq(t) + Ff(t), \qquad (6)$$

where

$$X = [C_{00}(t), \cdots, C_{M0}(t), C_{01}(t), S_{01}(t), \cdots, C_{MN}(t), S_{MN}(t)]^{\mathrm{T}}. \qquad (7)$$

Here, M, Γ, and K are matrices of the dimension $[(p+1)(2q+1)] \times [(p+1)(2q+1)]$; Q is the column vector showing the locations of the lateral cutting force, which is given by equation (1); F is matrix of the dimension $[(p+1)(2q+1)] \times K_c$ showing the locations of the control forces.

Equation (6) is rearranged in the state equation as

$$\dot{x}(t) = Ax(t) + Bu(t), \qquad (8)$$

where

$$x = \begin{bmatrix} X \\ \dot{X} \end{bmatrix}, u = \begin{bmatrix} q(t) \\ f(t) \end{bmatrix}, \qquad (9)$$

$$A = \begin{bmatrix} \mathrm{o} & I \\ -M^{-1}K & -M^{-1}\Gamma \end{bmatrix}, \qquad (10)$$

$$B = \begin{bmatrix} \mathrm{o} & \mathrm{o} \\ M^{-1}Q & M^{-1}F \end{bmatrix}. \qquad (11)$$

The displacement of the blade is obtained from the equation.

$$w(r, \eta, t) = Cx(t), \qquad (12)$$

where

$$C = [R_{00}(r), \cdots, R_{M0}(r), \cos(\eta)R_{01}(r), \sin(\eta)R_{01}(r), \cdots, \cos(N\eta)R_{MN}(r), \sin(N\eta)R_{MN}(r), 0 \cdots 0]. \qquad (13)$$

3. Numerical Results and Discussions

Numerical results that follow are for a S-2 blade cutting a 20.32cm (8″) diameter silicon ingot. The physical parameters of the blade measured are given in Table 1. Here,

Table 1 Physical parameters of slicing blade.

a'	0.3925 m	ν	0.28
a	0.3805 m	ρ	7.84×10^{3} kg/m^3
b	0.1525 m	E	1.63×10^{11} N/m^2
h	0.18×10^{-3} m	σ_0	4.48×10^{8} N/m^2

σ_0 is the initial radial tension at the outer periphery ($r = a'$) that was applied to the blade so that the inner hole of the blade is increased by Δb = 1mm.

3.1 Warp of the blade subjected to cutting force

An assumption is made that the blade is deformed laterally by the reaction force $L_z(\eta_0)$ from the ingot. It is said in general that the lateral cutting force is proportional to the length of cutting edge as shown in Fig. 2. In the following analysis, L_z is assumed proportional to the length of cutting edge, that is, the contact angle between the blade and the ingot.

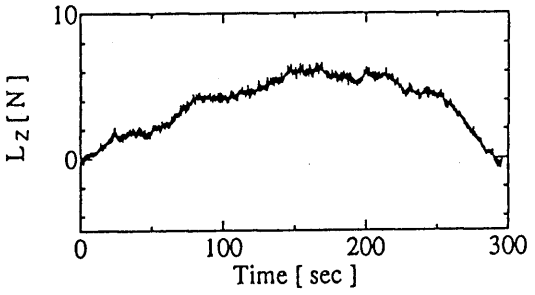

Fig.2 The lateral cutting force, L_z, as measured in an actual cutting process.

The contact angle η_0 is calculated analytically from the next equation as a function of the cutting depth of ingot x_I:

$$\eta_0(x_I) = \cos^{-1}\left[1 - \frac{x_I(2a_I - x_I)}{2b(x_I - a_I + b)}\right], \qquad (14)$$

where a_I is the radius of ingot. When the lateral cutting force acting on the blade is assumed proportional to η_0, the whole lateral cutting force is represented by

$$L_z = A\eta_0(x_I)/\eta_{0MAX}, \qquad (15)$$

where the maximum contact angle between the blade and the ingot is calculated as $\eta_{0MAX} = 41.78°$, while the average of maximum lateral reaction forces at this contact angle was measured $A = 4.02$ N for the sawblade cutting the 8″diameter ingot. On the other hand though the contact angle also changes as a function of the cutting depth, this angle is assumed constant($|\eta| \leq 30°$). The L_z is approximated by a set of concentrated forces that are distributed uniformly over the arc $|\eta| \leq 30°$ along the inner periphery of blade ($r = b$). Thus $q(t)$ in the equation (1) is given as

$$q(t) = L_z(t)/K, \tag{16}$$

Here, L_z is the magnitude of total axial cutting force, and K is the number of concentrated forces assumed. In the calculation that follows, the number of concentrated forces was assumed $K = 100$.

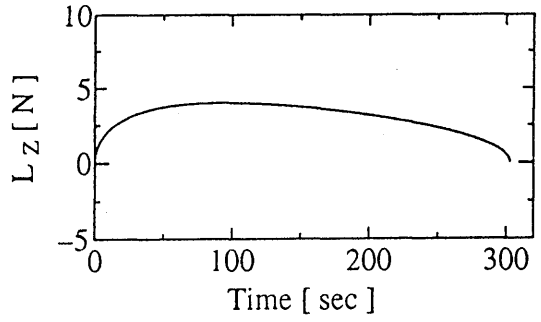

(a) Cutting force as predicted with the analytical model

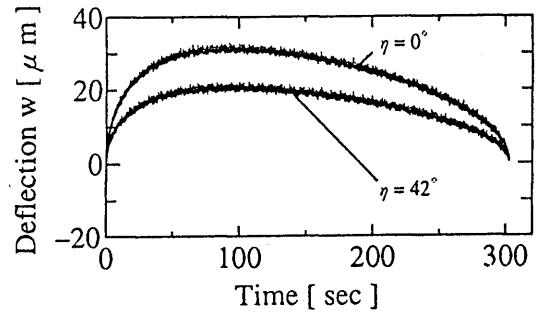

(b) Deflection at the tip of blade based on the predicted cutting force

Fig.3 Cutting force and the warp of blade without control force.

Figure 3 shows the cutting force L_z applied to the blade cutting the ingot and the deflection at the inner edge ($r = b$) without the control forces. Figure 3(a) shows the whole cutting force L_z calculated from equation(15). Figure 3(b) shows the deflection at the angles $\eta = 0°, 42°$ along the tip ($r/a = 0.401$) of blade subjected to L_z. It is found that the sign of the deflection is plus during the wafering and the deflection at $\eta = 0°$ is bigger than that one at $\eta = 42°$. As a result, the wafer produced becomes like a bowl. As observed from Fig. 3(b), the maximum of the deflection at the center of cutting edge is about 30μm, and it is necessary to suppress the deformation of the blade.

3.2 Warp Control of Blade

In the following analysis, two control schemes are investigated in detail that make the rotating blade flat. In both schemes, the control forces are applied to the blade symmetrically with respect to $\eta = 0°$. In the first scheme, a pair of concentrated control forces are applied to the blade ($K_c = 2$). In the second scheme, two additional control forces are further applied to the blade in the same circle ($K_c = 4$) so that a pair of control moments are applied to the blade in the circumferential direction.

It is well known that a control system becomes stable by using the feedback force in the integral control algorithm when the response of the blade is quasi-static. $f(t)$ in the equation (6) is multi-input and the control force f_j is represented by

$$f_j(t) = -G_I \int_0^t w_j(\tau) d\tau, \tag{17}$$

where G_I is non-dimensional integral gain. Further, the discretized equation of the above equation is

$$f_j(i) = -G_I \sum_{k=1}^{i} [w_j(k) + w_j(k-1)]/2. \tag{18}$$

Figure 4 shows the diagram of this control system to reduce warp of the blade. The transfer function $H(z)$ in the figure is the lowpass filter to remove high frequency component of feedback signal. That is given by

$$\begin{aligned} H(z) &= \frac{1}{N}(1 + z^{-1} + \cdots + z^{-(N-1)}) \\ &= \frac{1 - z^{-N}}{N(1 - z^{-1})}, \end{aligned} \tag{19}$$

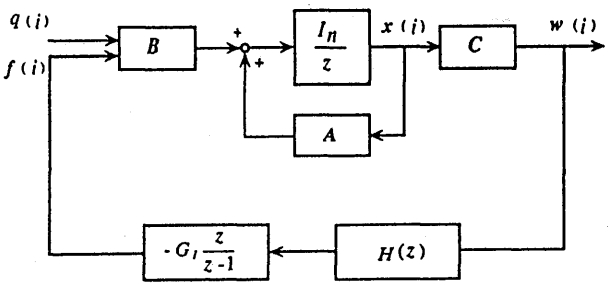

Fig.4 The control system used to reduce warp of blade.

where z^{-1} is the operator which means the time delay of one period. N in equation (19) is $N = 20$ in the following calculation.

The scheme where two control forces are applied to the blade is studied first. The locations of the control forces are examined that do not interfere with the path of the sliced ingot. The locations of the two forces on the blade are represented by a parameter $L(r/a, \pm\eta)$.

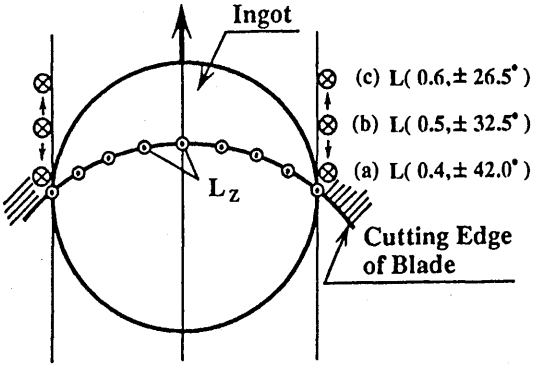

Fig.5 Three sets of control-force location on the blade.

Figure 5 shows three cases of the control forces applied to the blade. The forces are shifted parallel to the path of the ingot. The arrowhead shows the cutting force L_Z acting on the edge from downside, while the arrowroot shows the control forces calculated from equation (18). Figure 6 shows the results of control corresponding to the control forces (a)–(c) in Fig. 5. It is observed that the deflection at the center of cutting edge becomes minimum when two control forces are applied to (b)$L(0.5, \pm 32.5°)$. When the point of application is set very close to the inner edge, the suppression of deflection at the cutting edge is difficult. This is due to the fact that the relative angular position of the two forces is increased as the control forces approach the cutting edge.

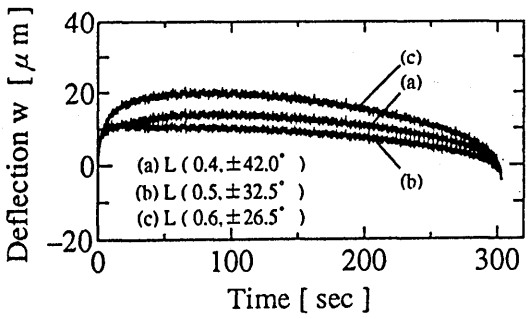

Fig.6 Blade deflection at the center of cutting edge for the three sets of control-force location.

The scheme of applying a pair of moments is studied next. The application points of the control forces are restricted to the location at which they do not interfere with the path of the processed ingot. In this scheme, four control forces are applied and a pair of control moments are produced on the same circle. The optimum radius where the control forces are applied is $r/a = 0.50$ according to the discussions given above. The locations of $f_1 - f_4$ are shown by the parameters L_1 and L_2. When L_2 is far from L_1, the control of deflection along the cutting edge will be not satisfactory. The circumferential position of L_2 is $\pm 40.0°$. Two additional control forces applied to L_2 are also calculated from equation (18). The integral gain for these additional forces is G_{I2}. The control argorithm used for F_2 is same argorithm (eqn.6.5) for F_1. Here is represent for G_{I2}. Figure 7 shows the effect on the blade deflection of control moments when the points of application of four control forces are L_1 (0.50, $\pm 32.5°$) and L_2(0.50, $\pm 40.0°$). Figure 7(a) shows the deflection at the center of cutting edge, while figure 7(b) shows the deflection at the point of application of the force $L_1(0.5, 32.5°)$. In both figures, the results obtained for no control, two points control and the case where a pair of control moments are applied to the blade are shown because of making a comparison between them. The control of deflection

at the point of application of the force is satisfactory as can be seen from Fig. (b). It is observed from Fig. (a) that the application of the moment is more effective than the simple lateral forces to reduce the deflection at the center of cutting edge.

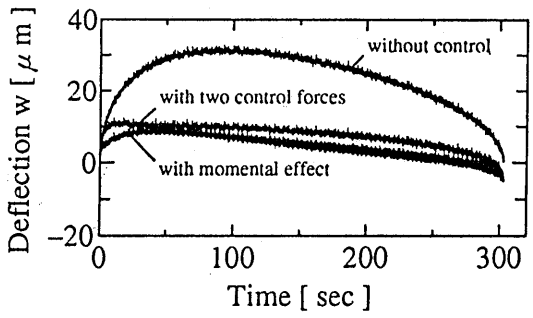

(a) $r/a = 0.401, \eta = 0°$

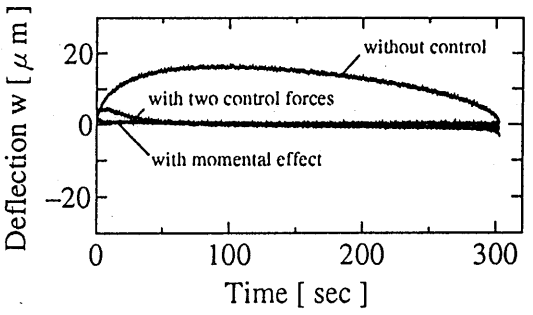

(b) $r/a = 0.5, \eta = 32.5°$

Fig.7 Suppression of warp by the moment effect. $L_1(0.5, \pm 32.5°)$, $L_2(0.5, \pm 40.0°)$, $G_I = G_{I2} = 100$.

Figure 8 shows the control forces corresponding to the control using a pair of moments in figure 7. The control forces in the figure are observed at $L_1(0.5, 32.5°)$ and $L_2(0.5, 40.0°)$. It is seen that the control forces at L_1 are applied to the blade in the opposite direction to the lateral cutting force. Those at L_2 are, on the other hand, applied to the blade in the same direction. Therefore, four control forces produce a pair of control moments. Further, the magnitude of control force applied to the blade is under output range of air pump which has already existed.

4. Conclusions

A theoretical analysis has been presented for the response of the rotating blade of wafer slicer subjected to the slicing load from the workpiece. The suppression of warp of blade has been studied in detail to produce a flat wafer. Results obtained show that the lateral control forces applied on the blade are effective to reduce the deflection of blade at the cutting edge. Further, it has been found that the scheme of applying four control forces that result in a pair of control moments on the blade is more effective than the scheme of applying just a pair of control forces, to make the cutting edgeof blade flat and to produce a flat wafer.

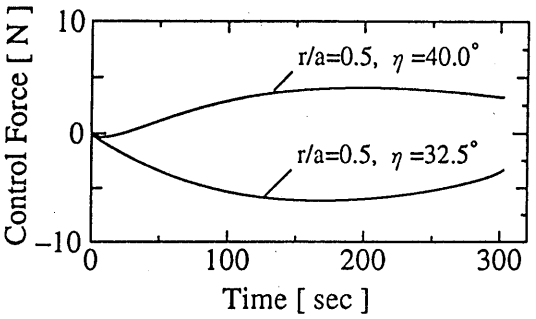

Fig.8 Control forces corresponding to the case of Fig. 7.

References

[1] Ellis, R. W. and Mote, C. D., Jr., A Feedback Vibration Controller for Circular Saws,ASME J. Dyn. Sys., Meas., Cont., 101, (1979), 44.

[2] Radcliffe,C.J. and Mote,C.D.,Jr., Identification and Control of Rotating Disk Vibration, ASME J. Dyn. Sys., Meas., Cont., 105, (1983), 39.

[3] Hutton,S.G., Chonan,S. and Lehmann,B.F., Dynamic Response of a Guided Circular Saw, J. Sound and Vib., 112-3, (1987), 527.

[4] Huang,S.C. and Hsu.B.S, Vibrations of a Spinning Annular Plate with Multi-Circular Line Guides, J. Sound and Vib., 164-3, (1993), 535.

[5] Chonan,S., Jiang,Z.W. and Yuki,Y., Stress Analysis of a Silicon-Wafer Slicer Cutting the Crystal Ingot, ASME J. Mech. Desi., 115, (1993), 711.

[6] Chonan,S., Jiang,Z.W. and Yuki,Y., Vibration and Deflection of a Silicon-Wafer Slicer Cutting the Crystal Ingot, ASME J. Vib. Acous., 115, (1993), 529.